



Published in final edited form as:

Nature. 2008 December 11; 456(7223): 819–823. doi:10.1038/nature07392.

DNA double strand breaks activate a multi-functional genetic program in developing lymphocytes

Andrea L. Bredemeyer^{*1}, Beth A. Helmink^{*1}, Cynthia L. Innes², Boris Calderon¹, Lisa M. McGinnis¹, Grace K. Mahowald¹, Eric J. Gapud¹, Laura M. Walker¹, Jennifer B. Collins², Brian K. Weaver¹, Laura Mandik-Nayak¹, Robert D. Schreiber¹, Paul M. Allen¹, Michael J. May³, Richard S. Paules², Craig H. Bassing^{4,5}, and Barry P. Sleckman¹

¹Department of Pathology and Immunology, Washington University School of Medicine, St. Louis, MO 63110

²Environmental Stress and Cancer Group, and NIEHS Microarray Group, National Institute of Environmental Health Sciences, Research Triangle Park, North Carolina

³School of Veterinary Medicine, Center for Childhood Cancer Research, Children's Hospital of Philadelphia, University of Pennsylvania School of Medicine

⁴Department of Pathology and Laboratory Medicine, Center for Childhood Cancer Research, Children's Hospital of Philadelphia, University of Pennsylvania School of Medicine

⁵Abramson Family Cancer Research Institute, Philadelphia, PA 19104

Abstract

DNA double strand breaks are generated by genotoxic agents and by cellular endonucleases as intermediates of several important physiologic processes. The cellular response to genotoxic DNA breaks includes the activation of transcriptional programs known primarily to regulate cell cycle checkpoints and cell survival^{1–5}. DNA double strand breaks are generated in all developing lymphocytes during the assembly of antigen receptor genes, a process that is essential for normal lymphocyte development. Here we demonstrate that these physiologic DNA breaks activate a broad transcriptional program. This program transcends the canonical DNA double strand break response and includes many genes that regulate diverse cellular processes important for lymphocyte development. Moreover, the expression of several of these genes is regulated similarly in response to genotoxic DNA damage. Thus, physiologic DNA double strand breaks provide cues that can regulate cell-type-specific processes not directly involved in maintaining the integrity of the genome, and genotoxic DNA breaks could disrupt normal cellular functions by corrupting these processes.

Users may view, print, copy, and download text and data-mine the content in such documents, for the purposes of academic research, subject always to the full Conditions of use:http://www.nature.com/authors/editorial_policies/license.html#terms

Correspondence to: Barry P. Sleckman, M.D., Ph.D., Department of Pathology and Immunology, 660 S. Euclid Ave., Campus Box 8118, Washington University School of Medicine, St. Louis, MO 63110, USA. Phone: 314-747-8235, Fax: 314-362-4096, email: Sleckman@immunology.wustl.edu.

*These authors contributed equally

Author Information

The microarray gene expression data has been deposited in NCBI's Gene Expression Omnibus accessible through GEO Series accession number GSE9024 (<http://www.ncbi.nlm.nih.gov/geo/query/acc.cgi?acc=GSE9024>).

The generation of complete antigen receptor genes in developing lymphocytes requires assembly of the second exon through the process of V(D)J recombination⁶. This process is initiated by the recombinase activating gene (Rag) endonuclease, composed of Rag1 and Rag2, which introduces DNA double strand breaks (DSBs) at the border of two gene segments and their flanking Rag recognition sequences (recombination signals or RSs)⁷. Rag cleavage occurs in cells at the G1 phase of the cell cycle, and the resulting pairs of coding and signal DNA ends are processed and joined by the non-homologous end-joining (NHEJ) pathway of DNA DSB repair, generating a coding joint and a signal joint respectively⁸. All developing lymphocytes must generate and repair several Rag DSBs as they assemble the genes encoding the heterodimeric B and T cell receptors.

The cellular response to genotoxic DSBs is initiated by the ataxia telangiectasia mutated (Atm) serine threonine kinase kinase^{1–3}. A central feature of this response is the activation of transcriptional programs, such as those initiated by p53, which primarily function to promote cell cycle arrest and apoptosis of cells with extensive, or persistent, DNA breaks⁹. Whether physiologic DSBs generally activate DSB responses that include these transcriptional programs has been unclear. In this regard, stabilization of p53 was observed only in NHEJ-deficient, and not wild type, thymocytes undergoing V(D)J recombination, suggesting that Rag DSBs may only activate transcriptional programs in a small fraction of developing lymphocytes where these breaks are not efficiently repaired and thus pose a hazard to the cell¹⁰. Indeed, the unopposed activation of p53 in response to transient Rag DSBs could lead to the unwanted apoptosis of developing lymphocytes that would have otherwise undergone successful antigen receptor gene assembly. Alternatively, all Rag DSBs could generally activate transcriptional pathways, including those that promote survival. In this regard, genotoxic DSBs have been shown to activate NFκB, and, although the genes that are regulated by NFκB in this setting have not been identified, in other settings NFκB regulates the expression of genes with anti-apoptotic activity^{5, 11, 12}. Moreover, NFκB promotes the expression of genes involved in diverse cell-type-specific processes, raising the intriguing possibility that genotoxic, and perhaps physiologic, DSBs activate genetic programs with broader cellular functions¹³.

Initially we wished to determine whether Rag DSBs are capable of activating NFκB. To this end, we generated several NHEJ-deficient (*Artemis*^{-/-}, *Ku70*^{-/-} and *Scid*) v-abl transformed pre-B cell lines, hereafter referred to as abl pre-B cells. G1 cell cycle arrest and Rag expression can be induced in these cells with the v-abl kinase inhibitor, STI571^{14, 15}. As these cells are NHEJ-deficient, Rag induction results in the accumulation of un-repaired DSBs at the immunoglobulin (Ig) light (L) chain κ locus (Supplementary Fig. 1, data not shown). These DSBs lead to activation of NFκB as evidenced by the increased nuclear translocation of NFκB (primarily p50/p65) in STI571 treated NHEJ-deficient (*Artemis*^{-/-}, *Ku70*^{-/-} and *Scid*) abl pre-B cells as compared to STI571 treated *Rag2*^{-/-} abl pre-B cells (Fig. 1a and Supplementary Fig. 2a and 2b). This NFκB activation was partially dependent on Atm as it was significantly diminished in *Artemis*^{-/-}:*Atm*^{-/-} abl pre-B cells and in *Artemis*^{-/-} abl pre-B cells treated with an Atm inhibitor (Fig. 1a and Supplementary Fig. 2c). As was observed for genotoxic DSBs, NEMO is required for the optimal activation of NFκB in response to Rag DSBs (Supplementary Fig. 2d) ^{12, 16, 17}.

To determine whether the activation of NF κ B, and possibly other transcription factors, by Rag DSBs leads to alterations in gene expression, we carried out gene expression profiling on three independently derived *Rag2*^{-/-} and *Artemis*^{-/-} abl pre-B cells treated with STI571 for 48 hours (Supplementary Fig. 3). These analyses revealed that the expression of 364 genes was changed 2-fold in all three *Artemis*^{-/-} abl pre-B cells relative to the mean expression level in the three *Rag2*^{-/-} cells (Fig. 1b, Supplementary Fig. 3a and Supplementary Tables 1, 2 and 3). A number of the gene expression changes were confirmed through quantitative RT-PCR and protein expression analyses (Fig. 1c and Supplementary Fig. 4 and 5). These changes are not due to Artemis deficiency *per se*, as they were also observed in response to Rag DSBs generated in *Ku70*^{-/-} and *Scid* (DNAPKcs-deficient) abl pre-B cells, but not in STI571-treated *Artemis*^{-/-}:*Rag2*^{-/-} abl pre-B cells (Supplementary Fig. 6). We conclude that Rag DSBs regulate the expression of a large cohort of genes. A significant portion of this cohort is dependent on the activation of Atm by Rag DSBs as evidenced by analyses of *Artemis*^{-/-}:*Atm*^{-/-} abl pre-B cells (Fig. 1, Supplementary Figs. 3–5 and 7 and Supplementary Tables 2 and 3). Remarkably, however, approximately half of the genes are Atm-independent, demonstrating that proteins other than Atm can initiate responses to Rag DSBs in G1-phase cells. Furthermore, analyses of *Artemis*^{-/-} abl pre-B cells expressing a dominant negative form of I κ B α (I κ B α -N), which inhibits NF κ B activation, revealed that 75 of the Atm-dependent gene expression changes were also NF κ B-dependent (Fig. 1b and 1c, Supplementary Fig. 3 and 4, and Supplementary Table 3). As only some of the Rag DSB-dependent genes are dependent on NF κ B, additional transcriptional pathways must be integrated into the Rag DSB response. Thus, Rag DSBs promote a broad genetic program, in part, through the activation of Atm and NF κ B.

A similar genetic program is activated by Rag DSBs in developing B cells *in vivo*. This is evidenced by gene expression profiling of purified B220⁺:IgM⁻ bone marrow B cells, which are primarily pre-B cells, from *Artemis*^{-/-} and *Rag1*^{-/-} mice expressing an IgH transgene (*Artemis*^{-/-}:*IgHtg* and *Rag1*^{-/-}:*IgHtg*, respectively) (Supplementary Fig. 8 and Supplementary Table 4). Of the 364 Rag-DSB-responsive genes identified through the analysis of *Artemis*^{-/-} abl pre-B cells, 109 exhibited significant changes in expression when comparing *Artemis*^{-/-}:*IgHtg* and *Rag1*^{-/-}:*IgHtg* pre-B cells (Fig. 1b, Supplementary Fig. 8 and Supplementary Tables 1–4). The asynchronous nature of Rag DSB induction in developing pre-B cells is likely responsible, in part, for the reduced magnitude and number of the gene expression changes in primary *Artemis*^{-/-}:*IgHtg* pre-B cells, as compared to the *Artemis*^{-/-} abl pre-B cells. Importantly, these gene expression changes do lead to significant increases in the expression of the proteins they encode (Fig. 2a and Supplementary Fig. 9). That these genes are Rag DSB-responsive was further demonstrated through the analysis of *Artemis*^{-/-}:*IgHtg* and *Rag1*^{-/-}:*IgHtg* bone marrow IL-7 pre-B cell cultures. Withdrawal of IL-7 from *Artemis*^{-/-}:*IgHtg*, but not *Rag1*^{-/-}:*IgHtg*, bone marrow IL-7 cultures leads to an increased accumulation of un-repaired IgL κ coding ends and a robust up-regulation in the expression of many of the genes that are regulated by Rag DSBs in abl pre-B cells (Fig. 2b, Supplementary Fig. 10 and data not shown)¹⁸. Together, these findings demonstrate that Rag DSBs activate a broad genetic program in developing pre-B cells. Importantly, these DNA breaks also promote gene expression changes in pro-B and pro-T cells, suggesting that

transcriptional programs are activated by Rag DSBs in all developing lymphocytes (Supplementary Fig. 11).

The genetic program induced by Rag DSBs includes genes that are active in multiple cellular processes. Several have functions that would be part of canonical DNA damage responses; for example, the anti-apoptotic proteins Pim2 and Bcl3 could antagonize pro-apoptotic pathways, such as those initiated by p53, promoting the survival of developing lymphocytes with Rag DSBs^{19–21}. Strikingly, this program also includes genes that have no known role in canonical DNA damage responses; instead, these genes participate in diverse processes, many of which are important for lymphocyte development and function. These include common γ chain, SWAP-70, Notch 1, CD69, CD40, CD80 (B7.1), and CD62L (L-selectin). Notably, CD62L, SWAP-70 and CD69 have known functions in lymphocyte homing and migration, suggesting that these gene expression changes could regulate the localization of developing lymphocytes with Rag DSBs^{22–26}. Indeed, we observed a biased accumulation of *Artemis*^{-/-} abl pre-B cells with Rag DSBs, as compared to *Rag2*^{-/-} abl pre-B cells, in the bone marrow after co-injection of these cells into Rag-deficient mice (Fig. 2c and Supplementary Fig. 12). A similar bias was not observed in the peripheral blood of these mice (Fig. 2c). Moreover, inhibition of Atm signaling in *Artemis*^{-/-} abl pre-B cells led to the diminished localization of these cells in the bone marrow (Supplementary Fig. 12c). Similar results were obtained from analyses of independently derived *Artemis*^{-/-} and *Rag2*^{-/-} abl pre-B cells (data not shown). Lymphocytes traverse different microenvironments as they develop in the thymus and bone marrow; our findings suggest that one of the functions of the Rag DSB-dependent genetic program may be to modulate this migration^{27–30}.

We have established that persistent Rag DSBs in NHEJ-deficient lymphocytes activate a diverse genetic program *in vitro* and *in vivo*. In wild-type lymphocytes, most Rag DSBs are repaired rapidly; thus, for this program to regulate processes that are generally important for development, it must also be initiated by these transient DSBs. In this regard, EMSA analyses did not reveal a marked increase in NF κ B activation in wild type abl pre-B cells undergoing V(D)J recombination; however, we reasoned that this analysis might not be sensitive enough to detect the activation of NF κ B in response to transient Rag DSBs (Supplementary Fig. 13). In agreement with this notion, we find that NF κ B-dependent, Rag DSB-responsive genes are up-regulated in an Atm-dependent manner in wild type developing B cells undergoing V(D)J recombination (Fig. 3a, Supplementary Figs. 9 and 14).

To directly determine whether transient Rag DSBs activate transcriptional pathways, we developed a sensitive single-cell assay for NF κ B activation. To this end, a retroviral reporter, pMSCV-NRE-GFP, that contains five tandem NF κ B responsive elements (NREs) driving expression of the green fluorescent protein (GFP) cDNA on the anti-sense strand was generated (Supplementary Fig. 15a). pMSCV-NRE-GFP was introduced into *Rag2*^{-/-} abl pre-B cells that contained the pMX-DEL^{CJ} retroviral V(D)J recombination substrate, hereafter referred to as *Rag2*^{-/-}:NRE cells (Fig. 3b and Supplementary Fig. 15)¹⁴. These cells do not express significant levels of GFP in response to STI571, but they do up-regulate

GFP in an ATM- and NFκB-dependent manner in response to DSBs induced by ionizing radiation (Fig. 3b and Supplementary Fig. 16).

To determine whether transient Rag DSBs activate NFκB, *Rag2*^{-/-}:*NRE* cells were transduced with a retrovirus encoding Rag2 (hereafter referred to as *Rag2*^{-/-}:*NRE*:R2 cells), which permits efficient V(D)J recombination after induction of Rag1 expression (Fig. 3c and data not shown). As STI571-treated cells are not dividing, GFP produced in response to transient Rag DSBs will persist, marking any cell that has activated NFκB (Fig. 3b and Supplementary Fig. 15c). Strikingly, after 48 hours of STI571 treatment, 53% of *Rag2*^{-/-}:*NRE*:R2 cells were GFP⁺ (Fig. 3b). This NFκB activation was *Atm*-dependent, as an *Atm* inhibitor abrogated GFP expression (Fig. 3b). If NFκB activation was stimulated by transient Rag DSBs, then there should be a higher level of completed rearrangements in the GFP⁺ cells. Indeed, PCR analyses revealed a 5-fold higher level of pMX-DEL^{CJ} rearrangement (coding joint, CJ, formation) in the GFP⁺ cells as compared to GFP⁻ cells (Fig. 3c). Moreover, the GFP⁺ cells exhibited increased expression of genes regulated by Rag DSBs, including *Pim-2*, *Bcl-3*, *CD40* and *CD69* (Figs. 3d and Supplementary Fig. 17). *CD69* expression in the GFP⁺ population was transient, similar to what was observed in response to persistent Rag DSBs (Fig. 3d and Supplementary Figs. 4a and 5b). Together, these data demonstrate that transient Rag DSBs generated during normal V(D)J recombination activate DNA DSB responses, including *Atm* and NFκB, which lead to the initiation of a diverse genetic program in all developing lymphocytes.

As physiologic Rag DSBs activate a broad genetic program, we reasoned that genotoxic DSBs may also activate components of this program in developing lymphocytes. Indeed, treatment of STI571-treated *Rag2*^{-/-} *abl* pre-B cells with either ionizing radiation (IR) or etoposide, which both generate DNA DSBs, led to the *Atm*-dependent induction of many genes that are also induced by Rag DSBs (Fig. 4a and b, Supplementary Fig. 18). Furthermore, treatment of bone marrow from *Rag1*^{-/-}:*IgHtg* mice with either ionizing radiation or etoposide leads to a B-cell-specific (B220⁺), *Atm*-dependent induction of *CD69* expression (Fig. 4c). These findings demonstrate that, in developing B cells, genotoxic DSBs can induce lymphocyte-specific gene expression changes that are normally induced by Rag DSBs.

We have shown that physiologic DNA DSBs generated during antigen receptor gene assembly activate a broad genetic program in developing lymphocytes. Importantly, this program is initiated by transient Rag DSBs that are rapidly repaired during normal V(D)J recombination in all developing lymphocytes. Thus, we propose that Rag DSBs provide cellular cues that regulate processes, such as migration and homing, that are integral components of normal lymphocyte development. As *Atm* is required to activate a portion of this Rag DSB-dependent genetic program, we expect that defects in the expression of these genes contribute to the lymphopenia observed in ataxia-telangiectasia.

Our findings establish for the first time that DNA DSBs generated during physiologic processes can regulate the cell-type-specific expression of genes that participate in functions not directly involved in maintaining genomic stability or suppressing malignant transformation. We speculate that DNA DSBs generated in other physiologic settings, such

as immunoglobulin class switch recombination, meiosis, and DNA replication, may have similar effects. Furthermore, genotoxic DSBs generated by agents such as ionizing radiation and chemotherapeutic drugs could corrupt normal cellular processes through the aberrant activation of these cell-type-specific genetic programs. Thus, the impact of DNA DSB responses on cell physiology and function is likely more pervasive than previously appreciated.

Methods Summary

Standard methodologies employed for cell culture, retroviral vector generation, western blotting, Southern blotting, EMSA, gene expression profiling, PCR and flow cytometry are described in detail in the Methods Section. All v-abl-transformed pre-B cell lines were generated from mice harboring the E μ Bcl-2 transgene as previously described¹⁴. Flow cytometric analyses were performed on a FACSCaliber (BD Biosciences) with the normalized geometric mean fluorescence intensity (MFI) calculated as the difference between the geometric mean fluorescence for the specific antibody and the isotype control. Flow cytometric cell sorting was performed using a FACSVantage (BD Biosciences). To generate pMSCV-NRE-GFP, the NF κ B responsive elements and TATA box from pNF- κ B-Luc (Stratagene) were amplified using the following oligonucleotides: pNRE-f: CCAAACATCAATGTATCTTATCATG; pNRE-r: TACCAACAGTACCGGAATGC. This PCR product was cloned upstream of a cDNA encoding enhanced GFP (Clontech) on the bottom strand of pMSCV containing an IRES upstream of the Thy1.2 cDNA. Gene expression profiling was performed using the Affymetrix 430 v2.0 mouse genome microarray. To assay abl pre-B cell localization, cells were treated for 48 hrs with STI571, labeled with 0.1 mM CFSE (Invitrogen) or 5 mM SNARF (Invitrogen) at 37°C for 15 minutes in PBS at 2–5 \times 10⁶/mL, washed 3 times, and re-suspended in DMEM at a concentration of 80 \times 10⁶/mL. Labeled cells were then mixed in a 1:1 ratio, and a total of 40 \times 10⁶ were injected into the tail vein of each Rag-deficient mouse. Bone marrow and peripheral blood was harvested 30–60 minutes post-injection and analyzed by FACS for presence of CFSE- and SNARF-labeled abl pre-B cells.

Methods

Mice

The *Atm*^{-/-}, *Scid*, *Ku70*^{-/-}, *Artemis*^{-/-}, VH147 IgH transgenic and E μ Bcl-2 transgenic mice have been described previously¹⁴, 31–33. Mice were bred and maintained under specific pathogen-free conditions at the Washington University School of Medicine and were handled in accordance to the guidelines set forth by the Division of Comparative Medicine of Washington University.

Cell culture

Three independently derived *Rag2*^{-/-} (R.1, R.2 and R.3), three independently derived *Artemis*^{-/-} (A.1, A.2 and A.3), two independently derived *Artemis*^{-/-}:*Atm*^{-/-} (AA.1 and AA.2) and individual *Scid* and *Ku-70*^{-/-} v-abl-transformed pre-B cell lines containing the E μ Bcl-2 transgene were generated. The three *Artemis*^{-/-}:I κ B α - N cells (A.3 N1, A.3 N2,

A.3 N3) were generated through standard transfection of the A.3 cells with a cDNA encoding an N-terminally truncated I κ B α (I κ B α - N)³⁴. Expression of the I κ B α - N protein in these cells was confirmed by western blotting. STI571 treatments were carried out with 3 μ M STI571, as previously described¹⁴. The KU-55933 Atm inhibitor (Sigma) was used at 15 μ M, the BAY-11-7085 inhibitor (Calbiochem) was used at 20 μ M, and etoposide was used at 5 μ M. Irradiation was carried out with a Cs¹³⁷ source, at doses of either 0.5 or 4 Gy.

Southern blotting

Southern blot analysis was performed as described previously^{14, 35}.

Western blotting and EMSA

Western blotting was carried out as described previously, using an antibody to Pim-2 (Santa Cruz, 1D12)³⁶. The secondary reagent was horseradish peroxidase (HRP)-conjugated goat anti-mouse IgG (Zymed). EMSAs were run as described previously, and analyzed using a Li-Cor Odyssey Infrared scanner³⁷. Supershifts were performed using anti-p50 and anti-p65 antibodies (Santa Cruz, sc-114 X and sc-372 X).

Gene expression profiling

All abl pre-B cells were harvested 48 hours following treatment with STI571. RNA was isolated using Qiagen RNeasy technology following the manufacturer's instructions. Gene expression analysis was conducted using Affymetrix Mouse Genome 2.0 GeneChip[®] arrays (Mouse 430 v2, Affymetrix, Santa Clara, CA). One μ g of total RNA was amplified as directed in the Affymetrix One-Cycle cDNA Synthesis protocol. Fifteen μ g of amplified biotin-cRNAs were fragmented and hybridized to each array for 16 hours at 45°C in a rotating hybridization oven using the Affymetrix Eukaryotic Target Hybridization Controls and protocol. Array slides were stained with streptavidin/phycoerythrin utilizing a double-antibody staining procedure and then washed using the EukGE-WS2v5 protocol of the Affymetrix Fluidics Station FS450 for antibody amplification. Arrays were scanned in an Affymetrix Scanner 3000 and data was obtained using the GeneChip[®] Operating Software (GCOS; Version 1.2.0.037). Data pre-processing, normalization, and error modeling was performed with the Rosetta Resolver system (Version 6.0)³⁸.

In order to identify differentially expressed genes between the *Rag2*^{-/-} and *Artemis*^{-/-} abl pre-B cells, an error-weighted analysis of variance (ANOVA) utilizing the Benjamini Hochberg false discovery rate was performed using Rosetta Resolver (www.rosettabio.com). At p-value 0.05, this analysis yielded 1578 probe sets. Fold changes were generated in Resolver, based on the ratio of each individual cell line relative to the average of the three *Rag2*^{-/-} cells with 100-fold being the maximum change that Resolver can report. Of the 1578 probes found using the ANOVA analysis, only those that had a fold-change ≥ 2.0 (not including anti-correlated genes) in all ratios for a given genotype were considered for further analysis. A Venn diagram of the resulting ANOVA and fold-change data sets for each genotype comparison to *Rag2*^{-/-} was then used to determine which expression changes were dependent on Atm and NF κ B.

For gene expression profiling of primary developing B cells, B220⁺ cells were isolated from *Rag1*^{-/-}:*IgHtg* and *Art*^{-/-}:*IgHtg* bone marrow using Mouse Pan B (B220) Dynabeads from Invitrogen. RNA was isolated using the Qiagen RNeasy Mini Kit. Microarrays were treated as described above for the abl pre-B cells. For the probe sets that were identified as being differentially regulated in response to Rag DSBs in the abl-pre-B cells, we compared the average expression in the two *Rag1*^{-/-}:*IgHtg* samples to the each of the two *Art*^{-/-}:*IgHtg* samples. The probe sets that were not anti-correlated and changed 1.5-fold in the average of these comparisons are included in Supplementary Table 4.

Flow cytometry

Flow cytometric analyses were performed using fluorescein isothiocyanate (FITC)-conjugated anti-CD45R/B220, allophycocyanin (APC)-conjugated anti-IgM, phycoerythrin (PE)-conjugated anti-CD40, PE-conjugated anti-CD62L, PE-conjugated anti-CD69, and the appropriate isotype controls (BD Biosciences).

Analysis of pMX-DEL^{CJ} rearrangement

PCR was carried out as described previously on 4-fold dilutions of genomic DNA14. IL-2 PCR primers were IMR42 and IMR43, and the product was probed with IMR042-2, all of which have been described previously¹. Primer sequences for pMX-DEL^{CJ} are as follows:

pA: CACAGGATCCCACGAAGTCTTGAGACCT

pB: ATCTGGATCCGTGCCGCCTTTGCAGGTGTATC

pD: AGACGGCAATATGGTGA

RT-PCR gene expression analysis

Quantitative real-time PCR (RT-PCR) was performed using a Stratagene Mx3000P real-time PCR machine and Platinum® SYBR® Green qPCR SuperMix-UDG (Invitrogen). PCRs were carried out using the following program: 95°C, 30 sec; 55°C, 60 sec; 72°C, 30 sec; 40 cycles. Relative expression is calculated as the difference between beta-actin expression (C1) and expression of the gene of interest (C2), using the following equation: relative expression = 2^{-(C1-C2)}. C is the PCR cycle where the product detection curve becomes linear. Primers are listed in Supplementary Table 5.

Supplementary Material

Refer to Web version on PubMed Central for supplementary material.

Acknowledgements

The authors thank Dr. Jeff Bednarski for critical review of the manuscript, Dr. Frederick W. Alt for generously providing us with the *Artemis*^{-/-} mice and Dr. Dean Ballard for providing us with the IκBα- N construct. This research is supported by NIH grant AI47829 and the Washington University Department of Pathology and Immunology (B.P.S.); the Department of Pathology and Center for Childhood Cancer Research of the Children's Hospital of Philadelphia, and the Abramson Family Cancer Research Institute (C.H.B.); the intramural research program of the NIH, National Institute of Environmental Health Sciences (R.S.P.). B.P.S. is a recipient of a Research Scholar Award from the American Cancer Society. C.H.B. is a Pew Scholar in the Biomedical Sciences. A.L.B. is supported by a post-doctoral training grant from the NIH.

References

1. Shiloh Y. ATM and related protein kinases: safeguarding genome integrity. *Nat Rev Cancer*. 2003; 3(3):155–168. [PubMed: 12612651]
2. Rouse J, Jackson SP. Interfaces between the detection, signaling, and repair of DNA damage. *Science*. 2002; 297(5581):547–551. [PubMed: 12142523]
3. Zhou BB, Elledge SJ. The DNA damage response: putting checkpoints in perspective. *Nature*. 2000; 408(6811):433–439. [PubMed: 11100718]
4. Innes CL, et al. ATM requirement in gene expression responses to ionizing radiation in human lymphoblasts and fibroblasts. *Mol Cancer Res*. 2006; 4(3):197–207. [PubMed: 16547157]
5. Rashi-Elkeles S, et al. Parallel induction of ATM-dependent pro- and antiapoptotic signals in response to ionizing radiation in murine lymphoid tissue. *Oncogene*. 2006; 25(10):1584–1592. [PubMed: 16314843]
6. Tonegawa S. Somatic generation of antibody diversity. *Nature*. 1983; 302:575–581. [PubMed: 6300689]
7. Fugmann SD, et al. The RAG proteins and V(D)J recombination: complexes, ends, and transposition. *Annu Rev Immunol*. 2000; 18:495–527. [PubMed: 10837067]
8. Rooney S, Chaudhuri J, Alt FW. The role of the non-homologous end-joining pathway in lymphocyte development. *Immunol Rev*. 2004; 200:115–131. [PubMed: 15242400]
9. Meek DW. The p53 response to DNA damage. *DNA Repair (Amst)*. 2004; 3(8–9):1049–1056. [PubMed: 15279792]
10. Guidos CJ, et al. V(D)J recombination activates a p53-dependent DNA damage checkpoint in scid lymphocyte precursors. *Genes Dev*. 1996; 10(16):2038–2054. [PubMed: 8769647]
11. Perkins ND. Integrating cell-signalling pathways with NF-kappaB and IKK function. *Nat Rev Mol Cell Biol*. 2007; 8(1):49–62. [PubMed: 17183360]
12. Huang TT, Wuerzberger-Davis SM, Wu ZH, Miyamoto S. Sequential modification of NEMO/IKKgamma by SUMO-1 and ubiquitin mediates NF-kappaB activation by genotoxic stress. *Cell*. 2003; 115(5):565–576. [PubMed: 14651848]
13. Gerondakis S, et al. Unravelling the complexities of the NF-kappaB signaling pathway using mouse knockout and transgenic models. *Oncogene*. 2006; 25(51):6781–6799. [PubMed: 17072328]
14. Bredemeyer AL, et al. ATM stabilizes DNA double-strand-break complexes during V(D)J recombination. *Nature*. 2006; 442(7101):466–470. [PubMed: 16799570]
15. Muljo SA, Schlissel MS. A small molecule Abl kinase inhibitor induces differentiation of Abelson virus-transformed pre-B cell lines. *Nat Immunol*. 2003; 4(1):31–37. [PubMed: 12469118]
16. May MJ, et al. Selective inhibition of NF-kappaB activation by a peptide that blocks the interaction of NEMO with the IkappaB kinase complex. *Science*. 2000; 289(5484):1550–1554. [PubMed: 10968790]
17. Wu ZH, Shi Y, Tibbetts RS, Miyamoto S. Molecular linkage between the kinase ATM and NF-kappaB signaling in response to genotoxic stimuli. *Science*. 2006; 311(5764):1141–1146. [PubMed: 16497931]
18. Grawunder U, et al. Expression of DNA-dependent protein kinase holoenzyme upon induction of lymphocyte differentiation and V(D)J recombination. *Eur J Biochem*. 1996; 241(3):931–940. [PubMed: 8944785]
19. Kashatus D, Cogswell P, Baldwin AS. Expression of the Bcl-3 proto-oncogene suppresses p53 activation. *Genes Dev*. 2006; 20(2):225–235. [PubMed: 16384933]
20. Amaravadi R, Thompson CB. The survival kinases Akt and Pim as potential pharmacological targets. *J Clin Invest*. 2005; 115(10):2618–2624. [PubMed: 16200194]
21. Hayden MS, Ghosh S. Signaling to NF-kappaB. *Genes Dev*. 2004; 18(18):2195–2224. [PubMed: 15371334]
22. Rosen SD. Ligands for L-selectin: homing, inflammation, and beyond. *Annu Rev Immunol*. 2004; 22:129–156. [PubMed: 15032576]

23. Feng C, et al. A potential role for CD69 in thymocyte emigration. *Int Immunol*. 2002; 14(6):535–544. [PubMed: 12039905]
24. Matloubian M, et al. Lymphocyte egress from thymus and peripheral lymphoid organs is dependent on S1P receptor 1. *Nature*. 2004; 427(6972):355–360. [PubMed: 14737169]
25. Shiow LR, et al. CD69 acts downstream of interferon-alpha/beta to inhibit S1P1 and lymphocyte egress from lymphoid organs. *Nature*. 2006; 440(7083):540–544. [PubMed: 16525420]
26. Pearce G, et al. Signaling protein SWAP-70 is required for efficient B cell homing to lymphoid organs. *Nat Immunol*. 2006; 7(8):827–834. [PubMed: 16845395]
27. Ladi E, Yin X, Chtanova T, Robey EA. Thymic microenvironments for T cell differentiation and selection. *Nat Immunol*. 2006; 7(4):338–343. [PubMed: 16550196]
28. Johnson K, et al. Regulation of immunoglobulin light-chain recombination by the transcription factor IRF-4 and the attenuation of interleukin-7 signaling. *Immunity*. 2008; 28(3):335–345. [PubMed: 18280186]
29. Tokoyoda K, et al. Cellular niches controlling B lymphocyte behavior within bone marrow during development. *Immunity*. 2004; 20(6):707–718. [PubMed: 15189736]
30. Nagasawa T. Microenvironmental niches in the bone marrow required for B-cell development. *Nat Rev Immunol*. 2006; 6(2):107–116. [PubMed: 16491135]
31. Rooney S, et al. Leaky Scid phenotype associated with defective V(D)J coding end processing in Artemis-deficient mice. *Mol Cell*. 2002; 10:1379–1390. [PubMed: 12504013]
32. Gu Y, et al. Growth retardation and leaky SCID phenotype of Ku70-deficient mice. *Immunity*. 1997; 7:653–665. [PubMed: 9390689]
33. Mandik-Nayak L, Racz J, Sleckman BP, Allen PM. Autoreactive marginal zone B cells are spontaneously activated but lymph node B cells require T cell help. *J Exp Med*. 2006; 203:1985–1998. [PubMed: 16880262]
34. Brockman JA, et al. Coupling of a signal response domain in I kappa B alpha to multiple pathways for NF-kappa B activation. *Mol Cell Biol*. 1995; 15:2809–2818. [PubMed: 7739562]
35. Ramsden DA, Gellert M. Formation and resolution of double-strand break intermediates in V(D)J rearrangement. *Genes Dev*. 1995; 9:2409–2420. [PubMed: 7557392]
36. Khor B, et al. Proteasome activator PA200 is required for normal spermatogenesis. *Mol Cell Biol*. 2006; 26:2999–3007. [PubMed: 16581775]
37. Weaver BK, Bohn E, Judd BA, Gil MP, Schreiber RD. ABIN-3: a molecular basis for species divergence in interleukin-10-induced anti-inflammatory actions. *Mol Cell Biol*. 2007; 27:4603–4616. [PubMed: 17485448]
38. Weng L, et al. Rosetta error model for gene expression analysis. *Bioinformatics*. 2006; 22:1111–1121. [PubMed: 16522673]

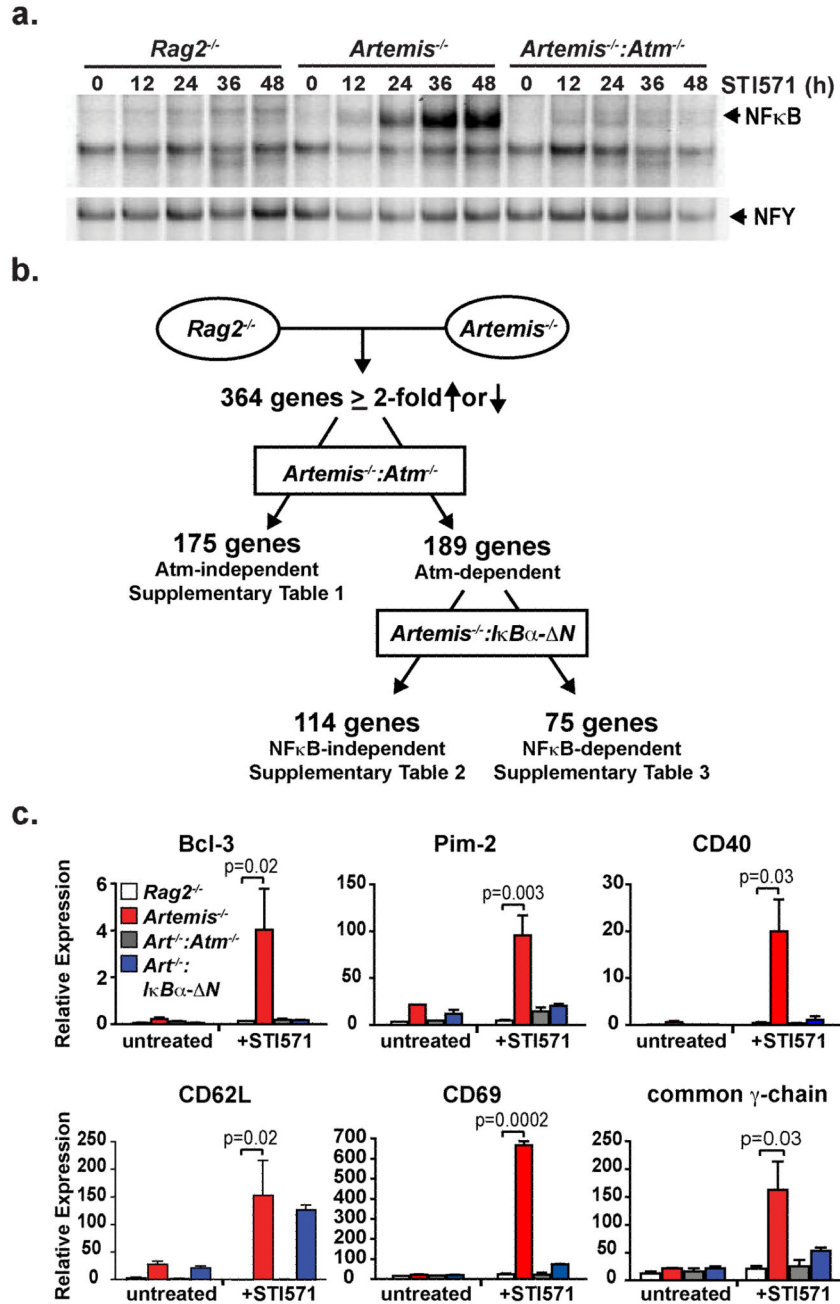


Figure 1. Rag DSBs activate a broad genetic program

(a) NF κ B EMSA of nuclear lysates from *Rag2*^{-/-}, *Artemis*^{-/-} and *Artemis*^{-/-}:*Atm*^{-/-} abl pre-B cells treated with STI571 for the indicated number of hours. NFY EMSA is shown as a control. Results are representative of three experiments. (b) Schematic of gene expression changes in response to Rag DSBs by microarray analyses. The data are reported in Supplementary Tables 1–3. (c) RT-PCR analysis of mRNA isolated from *Rag2*^{-/-} (white bars), *Artemis*^{-/-} (red bars), *Artemis*^{-/-}:*IκBα-ΔN* (blue bars) and *Artemis*^{-/-}:*Atm*^{-/-} (grey

bars) abl pre-B cells treated with STI571 for 0 or 48 hours. Mean and standard deviation from two experiments. P values calculated using a one-tailed t-test.

Author Manuscript

Author Manuscript

Author Manuscript

Author Manuscript

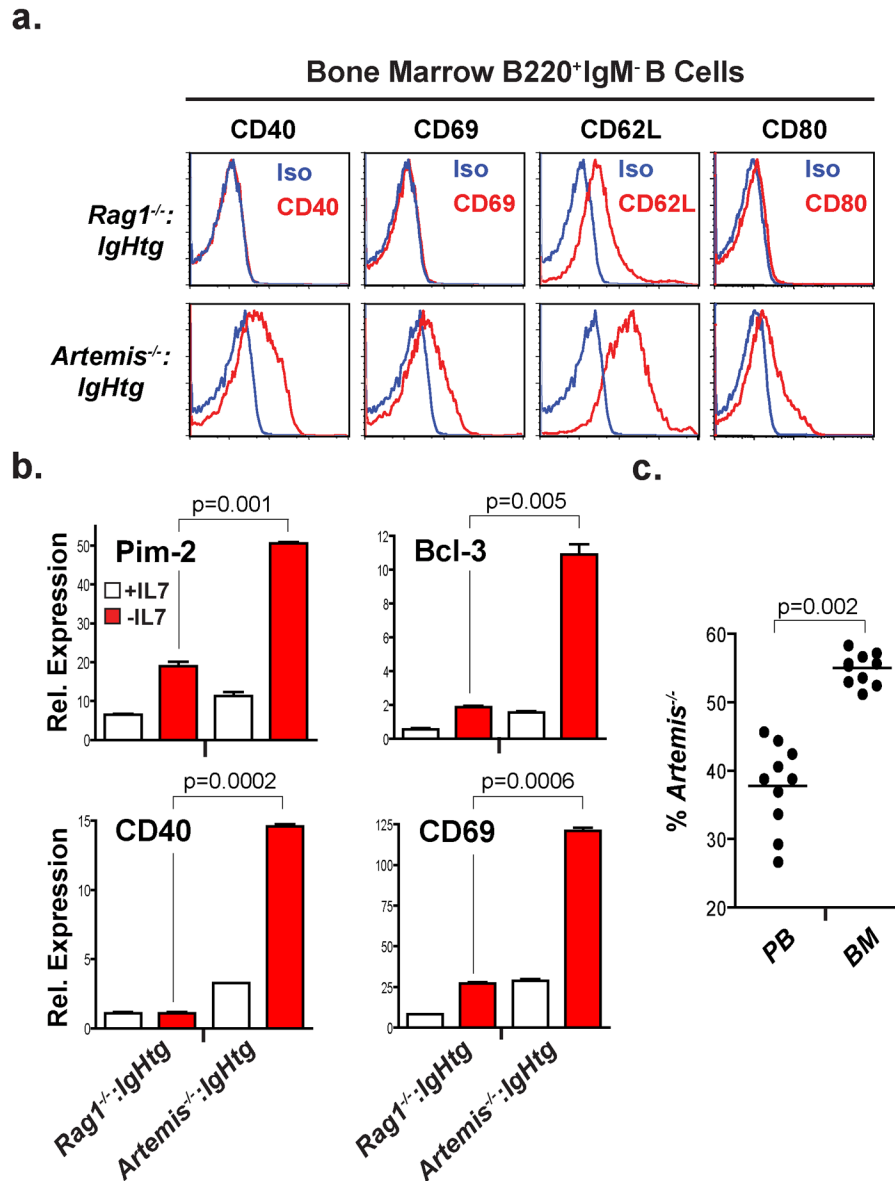


Figure 2. Rag DSB-dependent gene expression changes in developing B cells *in vivo*
(a) Flow cytometric analyses of CD40, CD69, CD80 and CD62L expression by B220⁺IgM⁻ bone marrow B cells (primarily pre-B cells) from *Rag1*^{-/-}:*IgHtg* and *Artemis*^{-/-}:*IgHtg* mice (gated in Supplementary Fig. 8). Histograms for specific antibodies (red) and isotype controls (blue) are shown. **(b)** RT-PCR of gene expression in bone marrow cultures derived from *Rag1*^{-/-}:*IgHtg* and *Artemis*^{-/-}:*IgHtg* mice before (+IL7, white bar) and 48 hours after (-IL7, red bar) the removal of IL7. Mean and standard deviation from two experiments. P values calculated using a one-tailed t-test. **(c)** Percentage of *Artemis*^{-/-} abl pre-B cells in the peripheral blood (PB) and bone marrow (BM) of Rag-deficient mice after co-injection of STI571-treated *Artemis*^{-/-} and *Rag-2*^{-/-} abl pre-B cells at a 1:1 ratio. The mean (line) of each set of mice analyzed is indicated and P values were calculated using a two-tailed Wilcoxon matched pairs test.

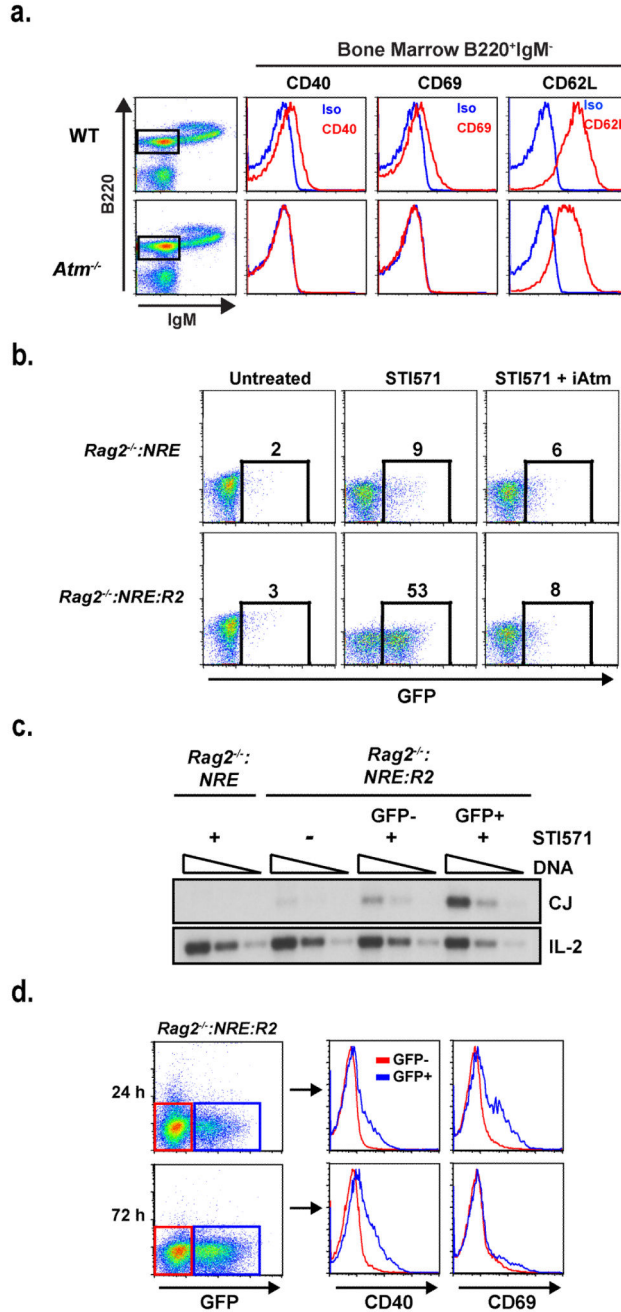


Figure 3. NFκB activation in response to transient Rag DSBs

(a) Flow cytometric analyses of CD40, CD69 and CD62L expression by B220⁺:IgM⁻ bone marrow B cells (gated cells in dot plot) from WT and *Atm*^{-/-} mice. Histograms for the specific antibodies (red) and isotype control (blue) are shown. (b) Flow cytometric analysis of GFP expression in *Rag2*^{-/-}:NRE and *Rag2*^{-/-}:NRE:R2 cells treated with STI571 for 48 hours in the presence or absence of the *Atm* inhibitor KU-55933 (iAtm). The percentage of GFP⁺ cells is indicated. Results are representative of three experiments. (c) *Rag2*^{-/-}:NRE and *Rag2*^{-/-}:NRE:R2 abl pre-B cells were un-treated (-) or treated with STI571 for 48

hours (+) and GFP⁺ and GFP⁻ *Rag2*^{-/-}:*NRE:R2* abl pre-B cells isolated by flow cytometric cell sorting. Serial 4-fold dilutions of genomic DNA from all cells was assayed for pMX-DEL^{CJ} rearrangement by PCR (see Supplementary Fig. 15b). Results are representative of two experiments. **(f)** Flow cytometric analysis of CD40 and CD69 protein expression on GFP⁺ (blue histograms) and GFP⁻ (red histograms) *Rag2*^{-/-}:*NRE:R2* cells treated with STI571 for 24 or 72 hours. Results are representative of two experiments.

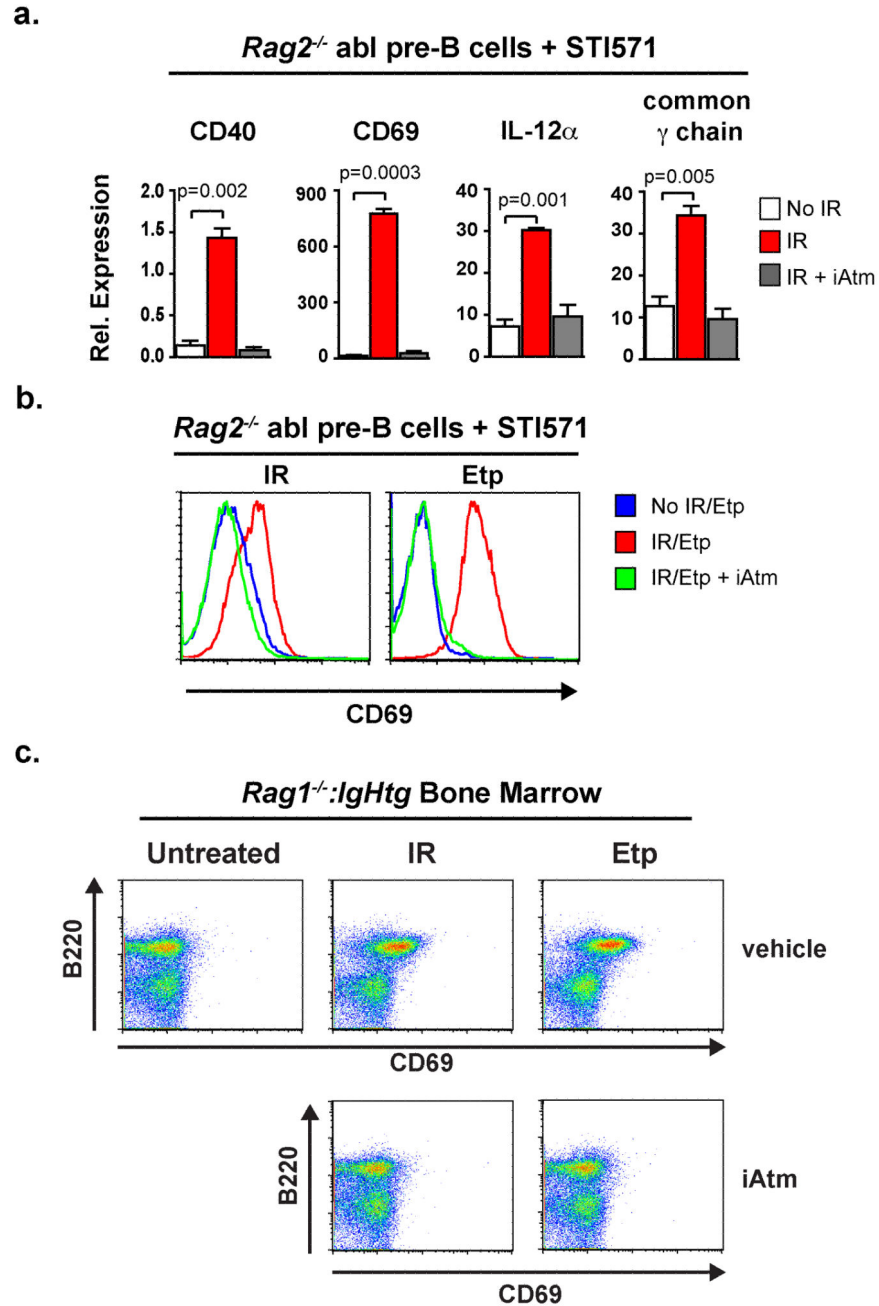


Figure 4. Genotoxic DSBs promote changes in expression of lymphocyte-specific genes
(a) RT-PCR analysis of gene expression in *Rag2*^{-/-} abl pre-B cells 2 hours after receiving 0 Gy (white bars) or 4 Gy of IR in the presence (grey bars) or absence (red bars) of the Atm inhibitor KU-55933 (iAtm). All cells were treated with STI571 for 24 hours prior to IR. Results are the mean and standard deviation from two experiments. P values were calculated using a one-tailed t-test. **(b)** Flow cytometric analysis of CD69 expression on STI571-treated *Rag2*^{-/-} abl pre-B cells treated with IR as described in (a) or 2 hours after being treated with 5 μ M etoposide (Etp). Results are representative of three experiments. **(c)** Flow cytometric

analysis of B220 and CD69 expression on bone marrow cells from *Rag1^{-/-}:IgHtg* mice 2 hours after irradiation (0.5 Gy) or etoposide treatment (5 μ M) in the presence or absence of the Atm inhibitor KU-55933. Results are representative of two experiments.

Author Manuscript

Author Manuscript

Author Manuscript

Author Manuscript